Catalysis Science & Technology

Accepted Manuscript

ROYAL SOCIETY OF CHEMISTRY

www.rsc.org/catalysis

Catalysis Science & Technology RSCPublishing

ARTICLE

Adsorption and Reaction Pathways of a Chiral Probe Molecule, S-glycidol on a Pd(111) Surface.

Cite this: DOI: 10.1039/xoxxoooooox

Mausumi Mahapatra[a] and Wilfred T. Tysoe[a]

Received ooth January 2012,
Accepted ooth January 2012

DOI: 10.1039/xoxxoooooox

www.rsc.org/

The chemistry of S-glycidol is studied on a Pd(111) surface using temperature-programmed desorption and reflection-absorption infrared spectroscopy to explore its suitability as a chiral probe molecule and to follow its reaction pathway. It is found that the majority of the S-glycidol desorbs intact with less than ~8% decomposing. Decomposition is initiated by forming an S-glycidate intermediate below ~200 K and this further reacts *via* C–O scission of the epoxy ring. This reaction is controlled by the stability of the carbocation intermediate to preferentially form an ethoxy aldehyde intermediate that thermally decomposes to desorb carbon monoxide, hydrogen and ethanol.

Introduction. The majority of pharmaceuticals are required to be in an enantiopure form necessitating either chiral separations of the racemate or the molecules to be synthesized in an enantiopure form. This is most often achieved using an organometallic catalyst containing chiral functional groups.[1-3] However, in this case, the product must be separated from the homogenous catalyst. This step could be avoided by using a chirally modified heterogeneous-phase catalyst. Unfortunately, this strategy has proven successful in only a very few cases.[4-8] A significant amount of work has been carried out to examine the surface chemistry of chiral adsorbates in order to provide insights into heterogeneous chiral catalysis.[9-34] However, the chiral expression of enantioselectivity requires an understanding of the interactions between the chiral modifier and prochiral reactant. One strategy for exploring such interactions is to use a chiral probe to measure the enantioselectivity of chirally modified surfaces from the relative coverages of enantiomers of the probe molecules on surfaces modified with adsorbates of the same or opposite chirality. Enantioselectivity is measured from the enantioselectivity ratio (ER) which is defined as the ratio of the coverages of the two enantiomers of the probe for the same coverage of the modifier; $ER=[\theta_R(Probe)/\theta_R(Modifier)]/([\theta_S(Probe)/\theta_R(Modifier)]$. This experiment, however, requires accurate coverage measurements. This has been carried out by using propylene oxide as a chiral probe,[35-40] which is particularly suitable for palladium surfaces since it undergoes negligible thermal decomposition, thereby allowing coverages to be measured using temperature programmed desorption. In addition, the infrared spectrum of propylene oxide on a Pd(111) surface exhibits reasonably intense vibrational modes, allowing infrared spectroscopy to also be used to monitor adsorbate coverages.[36] Propylene oxide contains only one potential hydrogen-bonding acceptor site (the epoxide oxygen), thereby limiting its use for investigating the stereochemistry of chiral interactions. Nevertheless, it has been demonstrated that the enantioselective adsorption of propylene oxide on R- or S-2-butanol-modified palladium surfaces is controlled by the hydrogen bonding between the –O–H group of 2-butanol and the epoxide oxygen of propylene oxide.[38] However, this approach would be rendered more versatile by being able to tune the location of hydrogen-bonding donor and acceptor sites on the probe molecule to provide a more detailed understanding of the nature and stereochemistry of the interactions that lead to enantioselectivity. An attractive strategy for achieving this would be to replace the methyl group in propylene oxide with a hydrogen donor/acceptor, by using a chiral probe such as glycidol (alternatively, oxiranylmethanol, 2,3–epoxy-1-propanol or 3-hydroxypropylene oxide) in which the $–CH_3$ group of propylene oxide is replaced by a $–CH_2–OH$ group. This molecule has been used to explore chiral recognition in the gas phase.[41, 42]

However, since alcohols undergo relatively facile deprotonation on Pd(111)[43, 44] the resulting potentially stronger binding of the glycidate to the surface may facilitate side reactions that hamper its use as a chiral probe molecule because of the associated difficulties in precisely measuring adsorbate coverages using temperature-programmed desorption. While such surface chemistry is anticipated to occur on Pd(111), if the extent of decomposition is minimal, it may still provide a useful chiral probe. In addition, insights into the reaction pathways of glycidol are useful for understanding non-selective pathways in the synthesis of ethylene oxide.[45, 46] Ethylene oxide decomposes on Pd(111) by an initial ring-opening reaction to form an oxametallacycle[47] that has been implicated as the central intermediate in the silver-catalyzed epoxidation of ethylene.[48, 49] Ethylene oxide forms from a reductive elimination of the oxametallacycle, which can also decompose by C–C or C–O bond scission or *via* a hydrogen-transfer reaction to produce acetaldehyde.[47] The desorption temperature of propylene oxide (~175 K[50]) on Pd(111) is lower than that of ethylene oxide (~255 K),[47] facilitating thermal decomposition in the latter case.

The goal of the work described in the following is two-fold. The first is to characterize the adsorption of glycidol on Pd(111) and to measure its extent of thermal decomposition to explore whether it is suitable as a chiral probe molecule and second, to monitor the decomposition pathways on Pd(111) by using a combination of temperature-programmed desorption and reflection-absorption infrared spectroscopy.

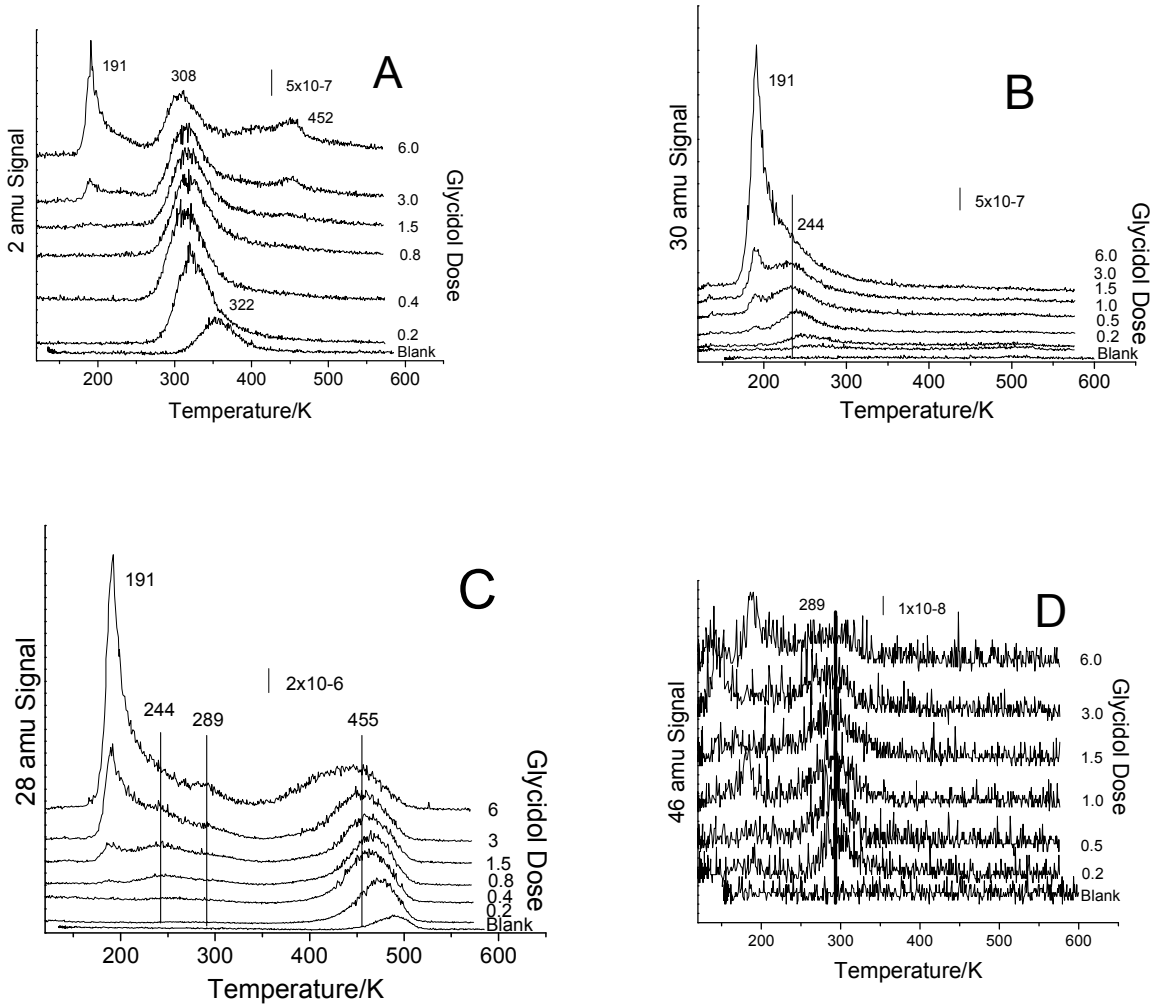

Figure 1: Temperature-programmed desorption profiles following the adsorption of S-glycidol on Pd(111) at ~90 K, as a function of S-glycidol dose (in Torr. min$\times 10^{-9}$), which are displayed adjacent to the corresponding desorption profile. The results were collected using a heating rate of 3 K/s and by monitoring (A) 2, (B) 30, (C) 28 and (D) 46 amu. Scale bars are included in each spectrum.

Experimental. The equipment used for these experiments has been described in detail elsewhere.[51] The TPD and RAIRS data were collected in different UHV chambers operating at base pressures of ~1×10^{-10} Torr following bakeout. In the TPD chamber, the Pd(111) single crystal was mounted to a carousel-geometry, x,y,z manipulator, which allowed the sample to be resistively heated to ~1200 K, and cooled to ~90 K by thermal contact to a liquid-nitrogen filled reservoir. TPD data were collected using a heating rate of ~ 3 K/s and the desorbing species were detected by a Dycor mass spectrometer, which was placed close to and in-line-of-sight of the sample front face. Infrared spectra were collected using a Bruker Vertex infrared spectrometer operating at a resolution of 4 cm^{-1}, using a liquid-nitrogen-cooled, mercury cadmium telluride detector, and spectra were typically collected for 1000 scans.

The Pd(111) substrate was cleaned using a standard procedure consisting of cycles of argon ion sputtering and annealing in 3×10^{-8}Torr of oxygen at 1000 K and the cleanliness was judged using Auger spectroscopy or TPD after dosing with oxygen, where the absence of CO desorption indicated that the sample was carbon free.

S-glycidol (Aldrich Chemical Co., 96%) was dosed onto the sample *via* a variable leak valve through a dosing tube directed towards the sample. Since this leads to an enhancement in the local pressure at the sample, which has not been calibrated, so that glycidol exposures are quoted in units of Torr.minutes, where the pressure is that measured by a nude ionization gauge in the chamber

Results and discussion. Experiments were carried out using S-glycidol. A series of TPD spectra collected as a function of S-glycidol exposure for a number of key masses (2 amu (hydrogen), 28 amu (glycidol and carbon monoxide), 30 amu (glycidol) and 46amu (glycidol and ethanol)) are displayed in Fig. 1. Hydrogen desorbs from a S-glycidol-covered surface (Fig. 1A), where the main desorption peak occurs between 322 and 308 K, close to the temperature for hydrogen desorbing from Pd(111),[52] indicating that the hydrogen is desorption-rate limited, implying that this arises from S-glycidol that has undergone some decomposition below this temperature. As indicated by the Blank desorption profile, a small amount of hydrogen adsorbs from the background. In addition, the

integrated intensity of the 2-amu feature decreases as the S-glycidol coverage increases, indicating that the extent of decomposition decreases at higher coverages. A sharp peak is also observed at ~191 K, due to the fragmentation of S-glycidol in the mass spectrometer ionizer. A decreasing hydrogen background is also observed at higher coverages, with a peak at ~452 K, indicative of the dehydrogenation of more strongly bound surface species. The corresponding 30 amu desorption profiles are shown in Fig. 1B and this mass is due to S-glycidol. A broad peak centred at ~250 K is detected at lower exposures, assigned to glycidol adsorbed on the Pd(111) surface. This peak shifts to lower temperatures (~ 244 K) at higher coverages suggesting some lateral interactions, or geometry changes occurring with increasing coverage.[50] A second S-glycidol feature appears at higher coverages with a peak temperature of ~191 K, which continually grows in intensity indicating that it is due to the formation of S-glycidol multilayers. The integrated intensities of the ~250 and 191-K features vary in exactly the same manner as a function of exposure, and the intensities at various masses also agree well with the mass spectrometer ionizer fragmentation pattern of S-glycidol, indicating that both features are due to S-glycidol desorption. The extent of S-glycidol decomposition can be gauged from the relative intensities of the hydrogen (2 amu) and S-glycidol. Accurately making this measurement requires values for ionization gauge sensitivities for hydrogen (~0.4) and S-glycidol, which is not available.[53] However, the sensitivity factor for propylene oxide is ~3.9, providing a likely lower limit for the sensitivity of glycidol. The result of this measurement suggests that less than ~8% of the S-glycidol decomposes during the desorption sweep on Pd(111). Thus, while the extent of S-glycidol decomposition is higher than for propylene oxide, it is still sufficiently low to allow TPD to be used to measure coverages on chirally modified surface to gauge chemisorptive enantioselectivity.

The corresponding 28 amu desorption profiles are plotted in Fig. 1C. The high-temperature feature at ~455 K is due to CO desorption arising from S-glycidol decomposition. The ~191 and 244 K peaks are assigned to mass spectrometer ionizer fragments of S-glycidol as discussed above, and an additional, relatively weak feature is detected at ~289 K at higher exposures. This is assigned to ethanol desorption as confirmed by the 46 amu desorption profile plotted in Fig. 1D, since it shows a peak at a similar temperature. Measurement of the signal at other masses confirms that the feature is due to ethanol desorption and no other desorption products were found.

It is clear that only a relatively small proportion of S-glycidol decomposes on Pd(111), and that this process is initiated by deprotonation to form an adsorbed glycidate. In order to gain insights into the surface reaction pathways, infrared spectra were collected of a Pd(111) surface saturated with S-glycidol at ~100 K, and then heated to various temperatures. The results of this experiment are displayed in Fig.2, where the annealing temperatures are displayed adjacent to the corresponding spectra. Essentially identical infrared spectra are measured at ~100 and 177 K, but the signals attenuate significantly on heating to ~187 K, coincident with multilayer S-glycidol desorption at ~191 K (Fig.1). All of the features in the low-temperature infrared spectra can be assigned by comparison with the spectrum of the pure material [54] and the frequencies are summarized in Table 1 along with their assignments. The close correspondence between the spectra of the adsorbed species and liquid S-glycidol confirms that pure S-glycidol adsorbs on the surface. This signal attenuates

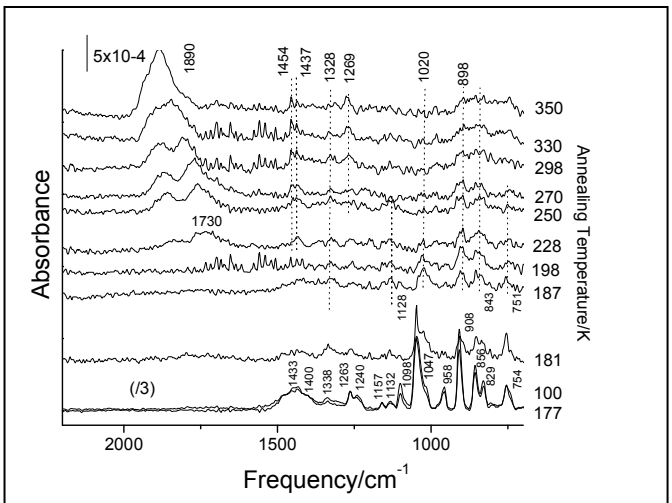

Figure 2: Reflection-absorption infrared spectra of 2×10^{-9} Torr. min of S-glycidol adsorbed on Pd(111) at 100 K and then heated to various temperatures, which are indicated adjacent to the corresponding spectrum.

significantly (note that the spectra collected at ~100 and 177 K have been attenuated by a factor of 3) when the sample is heated to ~187 K consistent with desorption of S-glycidol multilayers (Fig. 1).

A number of relatively weak features are detected as the temperature increases from ~197 to ~228 K (indicated on Fig. 2) at 751, 843, 898, 1020, 1128, ~1269, and 1328 cm^{-1}, with a broad feature at ~1430 K. The frequencies correspond rather closely to those for molecular S-glycidol and the frequencies for the features within the sample temperature range from ~197 to 228 K are indicated in parentheses in Table 1. Note that heating to above this temperature results in the appearance of a broad featured centred at ~1730 cm^{-1} that increases in frequency at higher annealing temperatures due to a C=O stretching mode.[55] The close correspondence between the modes found after heating to between ~187 and 228 K indicates that the S-glycidol molecular backbone remains intact. However, evidence for deprotonation is provided by the absence of the intense ~1047 cm^{-1} mode observed in the low-temperature spectra and the attenuation of the ~1433cm^{-1} feature. In this case, the mode appearing at ~1020 $cm^{-1}$is due to a shift in the C-O stretching mode (from ~1098 cm^{-1})[36] due to the formation of a S-glycidate. The spectral changes are therefore consistent with S-glycidol deprotonation at ~190 K as molecular S-glycidol desorbs.

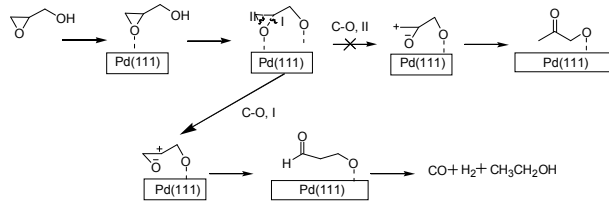

Scheme 1: A schematic illustration of the reaction pathways of S-glycidol on Pd(111).

Based on the chemistry found previously for epoxides on Pd(111),[47, 50] it is anticipated that ring opening should occur at ~220 K and should be accompanied by a hydrogen transfer reaction to form an aldehyde or ketone, consistent with the detection of C=O stretching modes at ~1730 cm^{-1} (Fig. 2).Depending on which of the C–O bonds cleaves in the epoxide ring, this can result in the formation of a ketone or an aldehyde. If the C-O bond indicated by I in Scheme 1 cleaves, this would result in the formation of a secondary carbocation, which will then undergo a facile hydrogen transfer to form an aldehyde-like intermediate. Alternatively, if cleavage occurs at C–O bond II, this would form a primary carbocation, which will undergo a similar hydrogen transfer reaction to form a ketone. Since secondary carbocations are more stable than primary carbocations, it is most probably that the epoxide ring cleaves at C–O bond I to preferentially form an aldehyde intermediate. This reaction pathway is consistent with the appearance of the C=O stretching modes at ~1730 cm^{-1}. The peaks at ~1440 cm^{-1} (1454 and 1437 cm^{-1}) are most likely due to CH_2 modes and the feature at ~1328 cm^{-1} is assigned to a symmetric methyl deformation mode.[55] A higher frequency mode appears at higher annealing temperature (>250 K). This feature appears at ~1890 cm^{-1}, due to adsorbed carbon monoxide, when the sample is heated to ~350 K, and dominates the spectrum. The resulting CO desorbs at ~450 K (Fig. 1C). This presumably arises from decomposition of the aldehyde group and the remainder of the molecule desorbs as a small amount of ethanol at ~289 K (Fig. 1D).[56] The reaction pathway for S-glycidol on Pd(111) is thus analogous to that found for ethylene oxide on Pd(111) [47] since decomposition occurs *via* C–O bond cleavage of the epoxide ring. However, in the case of the non-equivalent C–O bonds in the stabilized glycidate species, the reaction pathway is controlled by the stability of the intermediate carbocation, which undergoes a hydrogen transfer reaction.

Vibrational Frequency/cm^{-1} Glycidol/Pd(111), 100-177(187-228) K	Liquid glycidol Frequency/cm^{-1}[54]	Assignment
3271	3420, vs, brd	O-H stretch
3062	3062, m	$\nu_a(CH_2)$(Ring)
3000	2999, s	ν_s(C-H and CH_2)(Ring)
	2999, s	ν_s (CH_2 (Ring) and C-H).
2923	2927, s	ν(CH_2 (methanol))
2870	2873, s	ν(CH_2 (methanol))
1433 (brd)	1427, s	δ(O-H+ Ring)
1400 (~1400)	1400, s	δ(CH_2 (methanol) + Ring)
1338 (1328)	1338, w	δ(O-H + CH_2(methanol))
1263 (1269)	1260, s	δ(CH(Ring))
1240	1233, sh	δ(CH_2 (methanol))
1157	1156, w	δ(CH_2 (Ring))
1132 (1128)	1133, m	δ(CH + CH_2 (Ring))
1098 (1020)	1098, s	ν(C-O stretch) + δ(C-H)
1047	1041, vs	δ(O-H +CH_2 (methanol)) + δ(CH_2 (Ring))
958	956, s	δ(CH (Ring))
908 (898)	905, vs	Ring breathing
856 (843)	848, s	ν_a(Ring)
829	832, s	
	797, m	
754 (751)	750, s	δ(Ring)

Table 1: Comparison of the vibrational frequencies pf S-glycidol on Pd(111) between ~100 and 177 K compared with the spectrum of liquid glycidol. The measured frequencies for sample temperatures between ~187 and 228 K are indicated in parentheses. The model assignments are also shown. sh, shoulder; v, very; s, strong; m, medium, brd, broad; w, weak; ν, stretch; δ, deformation.

Conclusions

S-glycidol adsorbs relatively strongly on Pd(111) and desorbs intact at ~244 K. A small fraction of the molecules undergo decomposition reaction which is initiated by the dehydrogenation of the glycidol to glycidate species below 200K. The S-glycidate intermediate further reacts *via* C–O bond scission in the epoxide ring to preferentially form an ethoxy aldehyde intermediate in a pathway that is controlled by the stability of the carbocation. This thermally decomposes to desorb hydrogen and carbon monoxide with a small amount of ethanol. However, comparing the desorption yield of S-glycidol with that of molecular hydrogen suggest than less than ~8% of the adsorbed S-glycidol decomposes suggesting that it is suitable as a chiral probe molecule.

Acknowledgements
We gratefully acknowledge support of this work by the U.S. Department of Energy, Division of Chemical Sciences, Office of Basic Energy Sciences, under grant number DE-FG02-03ER15474. We thank John Kestell for useful discussions.

Notes and references
[a]Department of Chemistry and Laboratory for Surface Studies, University of Wisconsin-Milwaukee, Milwaukee, WI 53211, USA.

1. W. S. Knowles, *Angewandte Chemie International Edition*, 2002, **41**, 1998-2007.
2. H. C. Kolb and K. B. Sharpless, in *Transition Metals for Organic Synthesis*, eds. M. Beller and C. Bolm, Wiley-VCH, Weinheim, Germany, 1998, vol. 2, pp. 243-260.
3. R. Noyori, *Angewandte Chemie International Edition*, 2002, **41**, 2008-2022.
4. Y. Orito, S. Imai and S. Niwa, *J. Chem. Soc. Jpn.*, 1979, 1118-1120.
5. Y. Orito, S. Imai, S. Niwa and Nguyengiahung, *Journal of Synthetic Organic Chemistry Japan*, 1979, **37**, 173-174.
6. Y. Orito, S. Imai and S. Niwa, *J. Chem. Soc. Jpn.*, 1980, 670-672.
7. T. Harada and Y. Izumi, *Chemistry Letters*, 1978, 1195-1196.
8. Y. Izumi, *Advances in Catalysis*, 1983, **32**, 215-271.
9. J. Williams, S. Haq and R. Raval, *Surface Science*, 1996, **368**, 303-309.
10. M. O. Lorenzo, S. Haq, T. Bertrams, P. Murray, R. Raval and C. J. Baddeley, *Journal of Physical Chemistry B*, 1999, **103**, 10661-10669.

11. R. Raval, *Cattech*, 2001, **5**, 12-28.
12. V. Humblot, S. Haq, C. Muryn, W. A. Hofer and R. Raval, *J. Am. Chem. Soc.*, 2002, **124**, 503-510.
13. E. M. Marti, S. M. Barlow, S. Haq and R. Raval, *Surface Science*, 2002, **501**, 191-202.
14. S. M. Barlow and R. Raval, *Surface Science Reports*, 2003, **50**, 201-341.
15. R. Raval, *Current Opinion in Solid State & Materials Science*, 2003, **7**, 67-74.
16. V. Humblot, S. M. Barlow and R. Raval, *Progress in Surface Science*, 2004, **76**, 1-19.
17. V. Humblot, S. Haq, C. Muryn and R. Raval, *Journal of Catalysis*, 2004, **228**, 130-140.
18. V. Humblot and R. Raval, *Applied Surface Science*, 2005, **241**, 150-156.
19. A. G. Mark, M. Forster and R. Raval, *ChemPhysChem*, 2011, **12**, 1474-1480.
20. M. Forster, M. S. Dyer, M. Persson and R. Raval, *J. Am. Chem. Soc.*, 2011, **133**, 15992-16000.
21. T. E. Jones, C. J. Baddeley, A. Gerbi, L. Savio, M. Rocca and L. Vattuone, *Langmuir*, 2005, **21**, 9468-9475.
22. T. E. Jones, M. E. Urquhart and C. J. Baddeley, *Surface Science*, 2005, **587**, 69-77.
23. T. E. Jones and C. J. Baddeley, *Journal of Physical Chemistry C*, 2007, **111**, 17558-17563.
24. M. Parschau, S. Romer and K. H. Ernst, *J. Am. Chem. Soc.*, 2004, **126**, 15398-15399.
25. M. Parschau, T. Kampen and K. H. Ernst, *Chemical Physics Letters*, 2005, **407**, 433-437.
26. K. H. Ernst, in *Supramolecular Chirality*, 2006, vol. 265, pp. 209-252.
27. B. Behzadi, D. Ferri, A. Baiker and K. H. Ernst, *Applied Surface Science*, 2007, **253**, 3480-3484.
28. K. H. Ernst, *Chimia*, 2008, **62**, 471-475.
29. F. Gao, Y. L. Wang, L. Burkholder and W. T. Tysoe, *Surface Science*, 2007, **601**, 3579-3588.
30. F. Gao, Z. J. Li, Y. L. Wang, L. Burkholder and W. T. Tysoe, *Surface Science*, 2007, **601**, 3276-3288.
31. F. Gao, Z. J. Li, Y. L. Wang, L. Burkholder and W. T. Tysoe, *Journal of Physical Chemistry C*, 2007, **111**, 9981-9991.
32. F. Gao, Y. L. Wang and W. T. Tysoe, *Journal of Physical Chemistry C*, 2008, **112**, 6145-6150.
33. L. Burkholder and W. T. Tysoe, *Surface Science*, 2009, **603**, 2714-2720.
34. J. A. Boscoboinik, Y. Bai, L. Burkholder and W. T. Tysoe, *Journal of Physical Chemistry C*, 2011, **115**, 16488-16494.
35. J. D. Horvath and A. J. Gellman, *J. Am. Chem. Soc.*, 2001, **123**, 7953-7954.
36. D. Stacchiola, L. Burkholder and W. T. Tysoe, *J. Am. Chem. Soc.*, 2002, **124**, 8984-8989.
37. D. Stacchiola, L. Burkholder and W. T. Tysoe, *J. Mol. Catal. A-Chem.*, 2004, **216**, 215-221.
38. F. Gao, Y. L. Wang, L. Burkholder and W. T. Tysoe, *J. Am. Chem. Soc.*, 2007, **129**, 15240-15249.
39. F. Gao, Y. L. Wang, Z. J. Li, O. Furlong and W. T. Tysoe, *Journal of Physical Chemistry C*, 2008, **112**, 3362-3372.
40. J. L. Sales, V. Gargiulo, I. Lee, F. Zaera and G. Zgrablich, *Catalysis Today*, 2010, **158**, 186-196.
41. N. Borho and M. A. Suhm, *Physical Chemistry Chemical Physics*, 2002, **4**, 2721-2732.
42. A. Maris, B. M. Giuliano, D. Bonazzi and W. Caminati, *J. Am. Chem. Soc.*, 2008, **130**, 13860-13861.
43. J. L. Davis and M. A. Barteau, *Surface Science*, 1987, **187**, 387-406.
44. F. Gao, Y. L. Wang, L. Burkholder, C. Hirschmugl, D. K. Saldin, H. C. Poon, D. Sholl, J. James and W. T. Tysoe, *Surface Science*, 2008, **602**, 2264-2270.
45. R. B. Grant and R. M. Lambert, *Journal of Catalysis*, 1985, **92**, 364-375.
46. R. B. Grant and R. M. Lambert, *Journal of the Chemical Society, Chemical Communications*, 1983, 662-663.
47. R. M. Lambert, R. M. Ormerod and W. T. Tysoe, *Langmuir*, 1994, **10**, 730-733.
48. S. Linic and M. A. Barteau, *J. Am. Chem. Soc.*, 2001, **124**, 310-317.
49. S. Linic and M. A. Barteau, *J. Am. Chem. Soc.*, 2003, **125**, 4034-4035.
50. V. Bustos, D. Linares, A. G. Rebaza, W. T. Tysoe, D. Stacchiola, L. Burkholder and G. Zgrablich, *Journal of Physical Chemistry C*, 2009, **113**, 3254-3258.
51. M. Kaltchev, A. W. Thompson and W. T. Tysoe, *Surface Science*, 1997, **391**, 145-149.
52. H. Conrad, G. Ertl and E. E. Latta, *Surface Science*, 1974, **41**, 435-446.
53. R. L. U. S. N. A. Summers and L. R. C. Space Administration, National Aeronautics and Space Administration ; [For sale by the Clearinghouse for Federal Scientific and Technical Information, Springfield, Virginia 22151], Washington, D.C., 1969.
54. H. M. Badawi and S. A. Ali, *Spectrochimica Acta Part A: Molecular and Biomolecular Spectroscopy*, 2009, **74**, 558-562.
55. N. B. D. L. H. W. S. E. Colthup, *Introduction to infrared and Raman spectroscopy*, Academic Press, N.Y.
56. S. T. Marshall, C. M. Horiuchi, W. Zhang and J. W. Medlin, *The Journal of Physical Chemistry C*, 2008, **112**, 20406-20412.

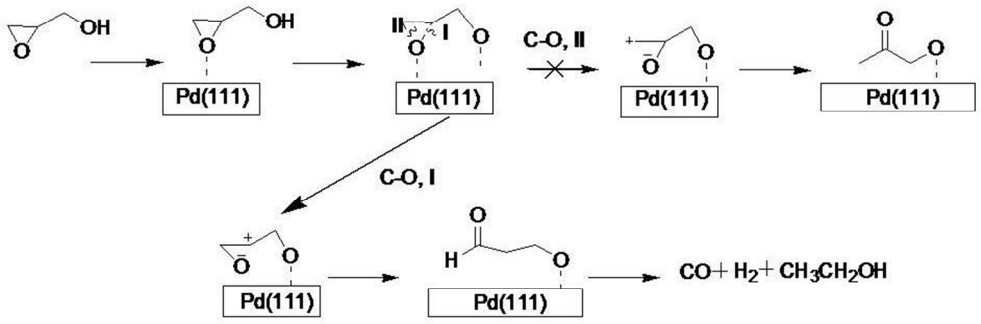

254x113mm (96 x 96 DPI)